Desalination and Water Treatment
www.deswater.com

24 (2010) 176–189
December

1944-3994/1944-3986
doi: 10.5004/dwt.2010.1497

Preparation of isoproturon and 2,4-dichlorophenoxy acetic acid imprinted membranes: Ion transport study

K.P. Singh[a*], R. Dobhal[b], R.K. Prajapati[c], Satish Kumar[a], Sanjesh[a], M.A. Ansari[d]

[a]*Biophysics and Nanotechnology Research Laboratory, CBSH, G. B. Pant, University of Agriculture & Technology, Pantnagar 263 145, Uttarakhand, India*
Tel. +919412632572; fax +915944234236; email: kps_biophysics@yahoo.co.in
[b]*Uttarakhand State Council for Science & Technology, Dehradun, Uttarakhand, India*
[c]*Department of Chemistry, D.J. College, Baraut 250611, India*
[d]*Department of Chemistry, Bipin Bihari (PG) Science College, Jhansi 284001, India*

Received 29 May 2009; accepted 13 May 2010

A B S T R A C T

Molecular imprinting technique is used for preparing molecularly imprinted polymer (MIP) membranes of desired recognition site, selectivity and porosity. The novelty of present work is to use a new approach for preparing imprinted monolith membrane, to study the effect of membrane porosity generated due to molecular imprinting on irreversible thermodynamical characteristics like membrane potential, ion transport, fixed charge density and permselectivity. It seems significant in developing membranes of desired selectivity and porosity for the removal and recognition of templates molecules. MIPs of potent herbicides isoproturon and 2,4-d were prepared by radical polymerization using methyl methacrylic acid (MAA) and ethylene glycol dimethacrylate (EGDMA) as functional monomer and cross linking agent. The polymer synthesis took place on a microporous support, which form hydrogen, covalent and ionic bonds with templates in order to form MIP membranes. The significance of this work is to discuss transport study of MIP membranes after creation of molecular recognition sites within the coated MIP. The MIP membranes were studied using theory of irreversible thermodynamics and by evaluating contact angle measurement, surface energy, ion transport study, perms electivity and fixed charge density of the membranes.

Keywords: Isoproturon; 2,4-D; Contact angle; Ion transport; Permselectivity; Fixed charge density

1. Introduction

Molecular imprinting is an easy and effective polymerization way to prepare synthetic materials able to mimic the molecular recognition in physical and biological systems. The synthesis of the artificial receptors was carried out by the imprinting procedure proposed by Wulff [1–3]. The imprinting polymerization consists of cross-linking of the functional monomers in the presence of a substrate template by radical polymerization followed by removal of the target molecules which is commonly called as templates. This procedure results in formation of the cavity imprints of a specific shape and a defined arrangement of functional groups on the polymer surface. On subsequent addition of the template molecules, recognition occurs by a combination

*Corresponding author

of reversible binding and shape complimentarily to the original print molecule. Because of the special recognition capacity, the molecular imprinting polymers (MIPs) have been widely investigated in the preparation of chiral chromatographic stationary phases, selective catalyst, and sensor components. MIP could be considered as appropriate alternatives to the biological/chemical receptors for its use as sensors principally because of their high stability. Biologically inspired (biomimetic) recognition properties are nowadays widely used in synthetic materials and structures by mimicking motif found in nature. The ability of many biomolecules to selectively recognize and bind to a specific substrate is a key process essential to every biological system [4–7].

Other methods for preparation of MIPs are based on in situ cross linking polymerization of functional and cross linker monomer yielding either self supported [8] or thin layer composite MIP membranes [9]. MIPs membranes have also been prepared by introducing molecular recognition sites into synthetic materials which do not initially possess any specific recognition. This method is called as ''alternative'' molecular imprinting [10] and developed during the last decades, which is analogous to the ''biological imprinting'' technique, which modifies the existing recognition function through the fixation of a conformation interaction with print molecule [11].

The present article focuses on the effect of membrane porosity generated by molecular imprinting on the ion transport and thermodynamical characteristics like membrane potential, ion transport, fixed charge density, permselectivity and contact angle measurements of developed membrane because these membranes are used in different kinds of applications [12]. The synthesis of stable polymeric membranes imprinted with potent herbicides Isoproturon and 2, 4-D templates was prepared through covalent, ionic, or hydrogen bonds with the corresponding functional monomers. Contact angle measurement of isoproturon and 2,4-D imprinted membranes was done for the determination of surface energy. Irreversible thermodynamical properties such as ion transport, permselectivity and fixed charge density of the imprinted membranes have been calculated for univalent, divalent and trivalent electrolytes by substituting the values of membrane potential in their respective equations from membrane potential data in order to know the effect of imprinted generated porosity of the MIP membranes.

2. Experimental section

2.1. Reagents

Unless otherwise mentioned, materials were obtained from commercial suppliers. Chemicals of Analytical reagent grade and solutions were prepared with deionized water. Isoproturon (3-*p*-cumenyl-1, 1-di-methyl urea) was purchased from Rallis India Ltd., Bombay. 2,4-Dichlorophenoxyacetic acid (2,4-D) was procured from Acros Organics Ltd. and used after recrystallized in alcohol thrice. Methacrylic acid (MAA) was procured from Serva (India). Ethylene glycol dimethacrylate (EGDMA) and *N*,*N*-dimethyl-*p*-toluidine (DMPT) were procured from Sigma Aldrich (India). Ethanol, toluene and benzyl alcohol were purchased from B.D.H. Benzoyl peroxide was procured from B.D.H., India and was recrystallized three times with chloroform.

2.2. Preparation of isoproturon and 2,4-D imprinted composite polymer membrane

MAA, EGDMA and isoproturon and were mixed with inert porogen and suitable templates (0.6% and 3.6% (w/w) and afterwards 2% (w/w) benzoyl peroxide were added. The mixture was degassed by argon within 10 min. To it 0.2 g DMPT was added. Circular Whatman filter paper no. 5 was soaked in the polymerization mixture and hung upright in a cylindrical glass container filled with argon. The polymerization was conducted overnight at room temperature. The non-imprinted control membrane was prepared without addition of the isoproturon templates.

Similarly 2,4-D imprinted composite polymer membrane was prepared as mentioned for isoproturon and the non-imprinted control membrane was prepared without addition of the 2,4-D templates.

2.3. Template removal and characterization of prepared MIP membranes

The removal of isoproturon and 2,4-D and characterizations of MIP membranes were characterized by UV-VIS spectrophotometer, Fourier transform infrared (FTIR) and scanning electron microscopy (SEM) prior to its application in transport studies.

2.3.1. UV–Visible spectrophotometer study of the membranes

The composite membranes were washed three times with ethanol to remove the print molecules and immersed in pure solvent before use. The filter paper soaked in the polymer mixture was placed in ethanol at 25 $\pm$ 0.1°C. The experimental and control membrane were dipped in 10 ml ethanol for one hour, respectively. After every hour the value of absorbance for isoproturon and 2,4-D were taken at λmax 240 and 340 nm using UV–Visible spectrophotometer, ECIL, India. This process was repeated when imprinted and

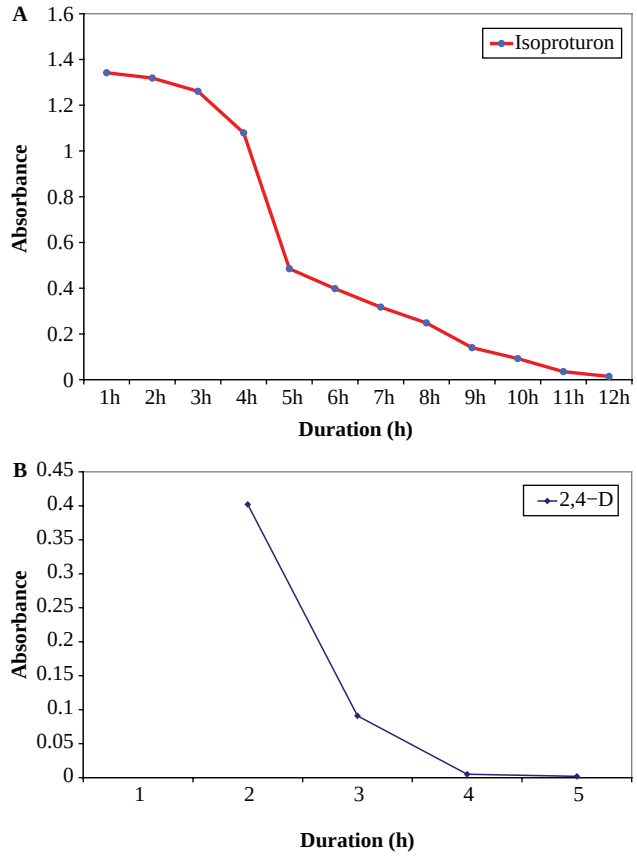

Fig. 1(a). Time series of isoproturon removal from MIP measured at 240 nm in UV–Visible spectrophotometer. (b). Time series of 2,4-D removal from MIP measured at 340 nm in UV–Visible spectrophotometer

non-imprinted membranes having the same value of absorbance. Absolute ethanol was used as blank.

The result obtained has been shown in Figs. 1(a) and1(b) which confirms the complete removal of template molecules from UM membrane after 12 h and leads to the formation of MIP membrane.

2.3.2. FTIR of MIP membrane with and without isoproturon and 2, 4-D template

The FTIR absorption spectra of the composite membrane prepared with and without of isoproturon and 2, 4-D templates were taken with FTIR (Nicollet). The absorption bands were recorded after five consecutive dipping of membrane in ethanol till the complete removal of template confirmed by UV–Visible spectrophotometer.

2.3.3. SEM

The prepared membranes were stored in NaN_3 until SEM study (Model JEOL JSM 840 SEM). MIP and non-imprinted membranes were analyzed at magnification 500 with resolutions 20, to record the morphology of membrane surface.

2.4. Contact angle measurement with isoproturon and 2,4-D imprinted membrane

The surface energy of membranes with templates and molecularly imprinted membranes, obtained after removal of isoproturon and 2,4-D were determined indirectly using contact angle measurements to compare effects produced in the unimprinted and printed membranes with the templates.

2.4.1. Geometric-mean equation

This approximation was first proposed by Girifalco and Good and later modified by Owens and Wendt [14]. According to Owens and Wendt, the surface energy of a solid can be determined using the following equation applied to two liquids:

$$(1+\cos\theta)\gamma_1 = 2\left(\gamma_s^d\gamma_1^d\right)^{1/2} + 2\left(\gamma_s^{nd}\gamma_1^{nd}\right)^{1/2}, \quad (1)$$

where the terms γ_s and γ_l are the surface free energies of the solid and pure liquid, respectively. The superscripts ''d'' and ''nd'' correspond to dispersive and non-dispersive contributions to the total surface energy, respectively. The contact angle, θ, obtained by the following equation was used in Eq. (1):

$$\theta = \cos^{-1}\left(\frac{\cos\theta_a + \cos\theta_r}{2}\right), \quad (2)$$

where θ_a and θ_r are the advancing and receding contact angle, respectively. By measuring the contact angles of two liquids on a membrane surface, two simultaneous equations will be obtained for Eq. (1), which can be solved for $\gamma_s{}^d$ and $\gamma_s{}^{nd}$. Consequently, by assuming the linear additivity of the intermolecular forces (i.e. dispersive and non-dispersive forces), the sum of the two components, $\gamma_s{}^d$ and $\gamma_s{}^{nd}$, should provide an estimate value of the total surface free energy. Owens and Wendt [14] employed water and methylene iodide as test liquids. Other liquid pairs have also been proposed in the literature [13–15].

2.4.2 Harmonic-mean equation

Alternatively, Wu proposed the use of the harmonic-mean expression in Young's equation for two liquids [13]. The following relationship was derived and employed to evaluate the total surface energy:

$$(1+\cos\theta)\gamma_1 = 4\left(\frac{\gamma_s^d\gamma_1^d}{\gamma_s^d+\gamma_1^d} + \frac{\gamma_s^{nd}\gamma_1^{nd}}{\gamma_s^{nd}+\gamma_1^{nd}}\right). \quad (3)$$

Table 1. Contact angles and surface energies of the unprinted (UM1 and UM2) and two molecularly imprinted Polymeric (MIP1, MIP2) membranes

	Water		Methanol		Geometric-mean approximation			Harmonic-mean approximation		
Membrane	θ_a	θ_r	θ_a	θ_r	γ_s^{nd} (mJ/m^2)	γ_s^{d} (mJ/m^2)	γ_s^{nd}/γ_s %	γ_s^{nd} (mJ/m^2)	γ_s^{d} (mJ/m^2)	γ_s^{nd}/γ_s %
UM1	86.2	68.8	51.3	37.8	6.6	30.5	17.8	14.6	21.2	40.8
MIP1	98.3	91.8	69.2	58.5	1.0	31.6	3.1	14.7	21.9	22.6
UM2	93.6	81.9	62.3	51.0	2.8	30.8	8.3	9.9	20.6	32.5
MIP2	98.0	86.3	66.7	54.5	1.5	31.7	4.5	7.7	21.5	26.4

2.5. Ion transport study

2.5.1. Measurements of membrane potentials of isoproturon and 2, 4-D MIP membrane

The membrane potentials were measured by setting a concentration cell of the type as shown below. The cell assembly was immersed in a thermostat water bath maintained at 25°C and all the experimental solutions of chemicals were also maintained on the same temperature. The electrochemical cell was comprised of two half cells of the following type. Each half cell contained a mechanical stirrer and saturated calomel electrodes attached to the multimeter (MASTECH M890D No. 00448814).

S.C.E Solution C1 Solution C2 S.C.E

Membrane

(C2 = 10 C1)

The membrane potential developed across the isoproturon and 2, 4-D MIP membranes were measured by a digital multimeter, respectively. The similar procedure was adopted with the solutions having varying concentration (1.0, 0.5, 0.2, 0.1, 0.05, 0.02, 0.01, 0.005, 0.002 and 0.001 M) of LiCl, NaCl, KCl, $MgCl_2$, $CaCl_2$, $AlCl_3$, FeCl3 electrolytes. The solutions of LiCl, NaCl, KCl, $MgCl_2$, $CaCl_2$, $AlCl_3$ and $FeCl_3$ were prepared in triple deionised water. The same electrolyte with different concentrations was used on both the sides of the membrane with $C_2 = 10C_1$ at $\gamma = 10$. The concentration ratio $\gamma = C_2/C_1$ was put equal to 10 throughout the experiment or in other words $C_2 = 10C_1$. The experiments were repeated a number of times with freshly prepared solutions of each of these electrolytes and the maximum potential values thus attained were recorded. The value of membrane potential across molecularly imprinted (isoproturon and 2,4-D imprinted membrane) at different concentration of 1:1,2:1 and 3:1electrolytes at 250°C are shown in Tables 2–4.

2.5.2. Study of transport ions with molecularly imprinted isoproturon and 2,4-D polymer membrane

The transport number of co-ions across MIP membrane can be calculated from the following expressions for 1:1 (LiCl, NaCl and KCl), 2:1 electrolyte ($CaCl_2$ and $MgCl_2$) and 3:1 electrolytes ($AlCl_3$ and $FeCl_3$), respectively, of varying concentration

$$\text{For } 1:1 \text{ electrolyte}: \ \Delta\varphi = (2t_+ - 1)\frac{RT}{F}\ln\frac{C_2}{C_1}, \qquad (4)$$

Table 2. Membrane potential measured across molecularly imprinted (isoproturon and 2,4-D composite membrane) polymer membrane at different concentration of 1:1 electrolytes at 25°C

		Membrane potential across MIP membrane in mV					
		LiCl		NaCl		KCl	
Sl. No	Concentration C_2/C_1 (mole l^{-1})	Isopro-turon	2,4-D	Isopro-turon	2,4-D	Isopro-turon	2,4-D
1	1/0.1	2.7	3.2	3.6	4.2	2.8	5.6
2	0.5/0.05	3.9	4.4	4.4	5.5	4.9	7.4
3	0.2/0.02	7.3	8.5	8.2	9.6	7.8	11.4
4	0.1/0.01	12.2	13.7	13.9	15.6	18.9	20.6
5	0.05/0.005	14.5	16.7	18.3	20.4	23.2	25.4
6	0.02/0.002	17.07	18.76	20.65	23	26.41	25.94
7	0.01/0.001	17.2	19	20.79	23.16	25.87	27.9

Table 3. Membrane potential measured across molecularly imprinted (isoproturon and 2,4-D composite membrane) polymer membranes potential at different concentration of 2:1 electrolytes at 25°C

Sl. No.	Concentration C_2/C_1 (mole/liter)	Membrane potential across MIP membrane in mV			
		$MgCl_2$		$CaCl_2$	
		Isoproturon	2,4-D	Isoproturon	2,4-D
1	1/0.1	11.40	13.10	12.30	14.40
2	0.5/0.05	12.50	14.00	14.40	16.70
3	0.2/0.02	14.20	16.00	18.90	21.00
4	0.1/0.01	18.90	20.20	26.70	28.20
5	0.05/0.005	26.60	28.80	29.80	33.00
6	0.02/0.002	30.50	33.00	36.40	38.40
7	0.01/0.001	27.10	28.30	32.80	35.00

$$\text{For } 2:1 \text{ electrolyte}: \ \Delta\varphi = \frac{RT}{F}\left(\frac{3\overline{t_+}}{2} - 1\right)\ln\frac{C_2}{C_1}, \qquad (5)$$

$$\text{For } 3:1 \text{electrolyte}: \ \Delta\varphi = \frac{RT}{F}\left(\frac{4\overline{t_+}}{3} - 1\right)\ln\frac{C_i}{C_e}, \qquad (6)$$

where $\Delta\Phi$ is membrane potential, C_1 and C_2 are concentration of electrolytic solutions filled in the two half of cells, t_+ is transport number of cations, R is gas constant; T is temperature and F Faraday constant. Transport number (t_+) derived from the observed membrane potentials for 1:1, 2:1 and 3:1 electrolyte concentrations at 25°C for MIP membrane are shown in Tables 5–7.

2.5.3. Study of permselectivity and fixed charge density with molecularly imprinted isoproturon and 2,4-D polymer membrane

The permselectivity (Ps) which is a measure of selectivity of membrane electrolyte systems has been calculated from membrane potential data

$$\frac{1}{t_+} = \frac{1}{(1-\alpha)} + \frac{(1+\beta-2\alpha\beta)(\gamma-1)\alpha}{2(1-\alpha)^2\ln\gamma}\left(\frac{\theta}{C_2}\right), \qquad (7)$$

where t_+ is a transference number of co-ions (Li^+, Na^+, K^+, Mg^{++} and Ca^{++} Al^{+++} and Fe^{+++}) in membrane phase. Applying Eq. (7) to Tables 5–7, in the value of permselectivity (Ps) and fixed charge density (Φx) in the concentrated solution range from the intercept and slope of the graph, for each combination of membrane electrolyte systems have been obtained.

The different values of α for LiCl, NaCl, KCl, $MgCl_2$ $CaCl_2$, $FeCl_3$ and $AlCl_3$ for each set of concentration are given in Tables 8–10 and these values are used for plotting the graph between $1/t_+$ and $1/C_2$.

The values of permselectivity are also related with the values of fixed charge density by the relations shown in Eq. (8)

$$\theta = \frac{2\cdot\bar{C}_S\cdot\mathrm{Ps}}{\sqrt{1-(\mathrm{Ps})^2}}, \qquad (8)$$

Table 4. Membrane potential measured across molecularly imprinted (isoproturon and 2,4-D composite membrane) polymer membranes potential at different concentration of 3:1 electrolytes at 25°C

Sl. No.	Concentration C_2/C_1 (mole/liter)	Membrane potential across MIP membrane in mV			
		$AlCl_3$		$FeCl_3$	
		Isoproturon	2,4-D	Isoproturon	2,4-D
1	1/0.1	15.30	17.10	17.90	19.20
2	0.5/0.05	17.70	19.20	16.30	18.20
3	0.2/0.02	23.30	25.80	27.80	29.10
4	0.1/0.01	26.90	28.50	34.50	36.40
5	0.05/0.005	42.40	43.60	47.90	49.20
6	0.02/0.002	49.70	51.42	54.90	55.68
7	0.01/0.001	43.40	45.40	43.70	47.10

Table 5. Transport number (t_+) derived from the observed membrane potentials for 1:1 electrolyte concentrations at 25°C for molecularly imprinted polymer membrane

Sl No.	Concentration C_2/C_1 (mole/liter)	LiCl		NaCl		KCl	
		Isopro-turon	2,4-D	Isopro-turon	2,4-D	Isopro-turon	2,4-D
1	1/0.1	0.52	0.527	0.530	0.535	0.529	0.547
2	0.5/0.05	0.53	0.537	0.537	0.546	0.541	0.56
3	0.2/0.02	0.56	0.527	0.569	0.58	0.566	0.596
4	0.1/0.01	0.603	0.616	0.617	0.63	0.66	0.674
5	0.05/0.005	0.62	0.64	0.66	0.703	0.69	0.715
6	0.02/0.002	0.64	0.657	0.672	0.69	0.723	0.719
7	0.01/0.001	0.63	0.66	0.676	0.69	0.719	0.736

Table 6. Transport number (t_+) derived from the observed membrane potential for 2:1 electrolyte concentrations at 25°C for MIP

Sl. No.	Concentration C_2/C_1 (mole/liter)	$MgCl_2$		$CaCl_2$	
		Isoproturon	2,4-D	Isoproturon	2,4-D
1	1.0/0.1	0.79	0.814	0.80	0.829
2	0.5/0.05	0.80	0.820	0.829	0.855
3	0.2/0.02	0.82	0.847	0.88	0.905
4	0.1/0.01	0.88	0.890	0.96	0.985
5	0.05/0.005	0.96	0.990	1.00	1.039
6	0.02/0.002	1.01	1.039	1.073	1.100
7	0.01/0.001	0.97	0.98	1.028	1.080

Table 7. Transport number (t_+) derived from the observed membrane potential at 3:1 electrolyte concentrations at 25°C for MIP membrane

Sl. No.	Concentration C_2/C_1 (mole/liter)	$AlCl_3$		$FeCl_3$	
		Isoproturon	2,4-D	Isoproturon	2,4-D
1	1/0.1	0.944	0.969	0.979	0.996
2	0.5/0.05	0.977	0.996	0.959	0.983
3	0.2/0.02	1.048	1.0806	1.106	1.121
4	0.1/0.01	1.121	1.115	1.191	1.207
5	0.05/0.005	1.292	1.307	1.362	1.373
6	0.02/0.002	1.373	1.406	1.451	1.449
7	0.01/0.001	1.304	1.325	1.305	1.347

Table 8. The values of $1/t_+$ and $1/C_2$ for LiCl, NaCl and KCl across molecularly imprinted (isoproturon and 2,4-D composite membrane) polymer membranes

Sl. No.	$1/C_2$		$1/t_+$ for LiCl		$1/t_+$ for NaCl			$1/t_+$ for KCl
	Isopro-turon	2,4-D	Isopro-turon	2,4-D	Isopro-turon	2,4-D	Isopro- turon	2,4-D
1.	1	1	1.923	1.897	1.886	1.869	1.89	1.828
2.	2	2	1.785	1.862	1.862	1.831	1.848	1.785
3.	5	5	1.658	1.748	1.757	1.724	1.766	1.677
4.	10	10	1.612	1.623	1.620	1.587	1.515	1.487
5.	20	20	1.562	1.562	1.514	1.422	1.449	1.398
6.	50	50	1.5625	1.522	1.492	1.449	1.383	1.390
7.	100	100	1.587	1.515	1.479	1.449	1.390	1.350

Table 9. The values of $1/t_+$ and $1/C_2$ for $MgCl_2$ and $CaCl_2$ across molecularly imprinted (isoproturon and 2,4-D composite membrane) polymer membranes

	$1/C_2$		$1/t_+$ for $MgCl_2$		$1/t_+$ for $CaCl_2$	
Sl. No.	Isoproturon	2,4-D	Isoproturon	2,4-D	Isoproturon	2,4-D
1.	1	1	1.26	1.228	1.25	1.206
2.	2	2	1.25	1.219	1.204	1.169
3.	5	5	1.219	1.1806	1.136	1.101
4.	10	10	1.136	1.123	1.042	1.015
5.	20	20	1.042	1.010	1.00	0.962
6.	50	50	0.990	0.969	0.931	0.909
7.	100	100	1.030	1.0202	0.972	0.925

where θ is fixed charge density, C_s is mean concentration of electrolyte and Ps is the permselectivity. The values of fixed charge density are summarized in Tables 14 and 15 and calculated by employing Eq. (8) for different values of permselectivity are given in Tables 11–13.

3. Results

3.1. FTIR of MIP membrane with and without isoproturon and 2,4-D template

FTIR absorption spectra of the composite membrane prepared with isoproturon template shows significant absorption bands on 3,334, 1,717, 1,635, 1,453, 1,314, 1,295, 1,155, 1,108, 1,027, 813, 697 and 593 nm (Fig 2(a)). In contrast absorption bands at 1,717, 1,295 and 813 are absent in imprinted membranes without template which allows confirming the removal of isoproturon (Fig. 2(b)). The absorption band at 1,717, 1,635 and 813 indicates the presence of the anilide bond, amide bond and aromatic system of isoproturon.

FTIR absorption spectra of the composite membrane prepared with 2,4-D template shows significant absorption bands on 3,333, 1,717, 1,314, 1,295, 1,158, 1,107, 1,029, 813, 697 and 593 nm (Fig. 3(a)). In contrast absorption bands at 1,717, 1,295 and 813 are absent in imprinted membranes without template which allows confirming the removal of 2,4-D (Fig. 3(b)).

3.2. SEM

The micrographs given in Figs. 4(a) and 4(b) show morphology of the isoproturon and 2,4-D imprinted MIP membrane. The surface morphology clearly indicates the porous structures even after template removal.

3.3. Calculation of surface energy from contact angles

Contact angles of water and methanol on the surface of the prepared non-imprinted and imprinted membranes were measured at room temperature using the contact angle meter Horizontal Beam Comparator (SCHERR ST TUMICO). Initial drops of about 2 μl were deposited on the membrane surface employing a tight syringe that was adjusted 0.5 mm above the membrane surface. The volume of the drop was slowly increased and decreased by adding the liquid to and subsequently withdrawing it from the surface using the syringe.

Direct measurements of the advancing contact angle reflect the hydrophobic character of the surface,

Table 10. The values of $1/t_+$ and $1/C_2$ for $AlCl_3$ and $FeCl_3$ across molecularly imprinted (isoproturon and 2,4-D composite membrane) polymer membranes

	$1/C_2$		$1/i_+$ for $AlCl_3$		$1/t_+$for $FeCl_3$	
Sl. No.	Isoproturon	2,4-D	Isoproturon	2,4-D	Isoproturon	2,4-D
1.	1	1	1.059	1.039	1.0214	1.004
2.	2	2	1.023	1.004	1.042	1.017
3.	5	5	0.954	0.925	0.904	0.892
4.	10	10	0.89	0.896	0.839	0.828
5.	20	20	0.773	0.765	0.734	0.728
6.	50	50	0.726	0.711	0.689	0.690
7.	100	100	0.766	0.754	0.766	0.742

Table 11. Values of $\log(C_1+C_2)/2$ and permselectivity for LiCl, NaCl and KCl electrolytes across molecularly imprinted (isoproturon and 2,4-D composite membrane) polymer membranes

			The values of permselectivity					
			LiCl		NaCl		KCl	
Sl. No.	Molar Conc.	$\log(C_1+C_2)/2$	Isopro-turon	2,4-D	Isopro-turon	2,4-D	Isopro-turon	2,4-D
1	1/1.0	−0.25	−2.25	−2.29	−2.27	2.28	2.18	1.655
2	0.5/0.05	−0.56	−2.92	−2.21	−2.28	−2.0	−2.098	−1.578
3	0.2/0.02	−0.95	−1.97	−2.29	−1.992	−2.06	−1.942	−1.473
4	0.1/0.01	−1.25	−1.76	−1.74	−1.79	−1.62	−1.54	−1.319
5	0.05/0.005	−1.56	−1.68	−1.58	−1.43	−154	−1.674	−1.259
6	0.02/0.002	−1.95	−1.61	−1.61	−1.54	−1.45	−1.38	−1.252
7	0.01/0.001	−2.25	−1.64	−1.58	−1.56	−1.40	−1.39	−1.228

Table 12. Values of $\log(C_1+C_2)/2$ and permselectivity for $MgCl_2$, $CaCl_2$ electrolytes across molecularly imprinted (Isoproturon and 2,4-D composite membrane) polymer membranes

			The values of permselectivity			
			$MgCl_2$		$CaCl_2$	
Sl. No.	Molar Conc.	$\log (C_1+C_2)/2$	Isoproturon	2,4-D	Isoproturon	2,4-D
1	1/0.1	−0.25	−1.092	−1.068	−1.075	−1.057
2	0.5/0.05	−0.56	−1.086	−1.067	−1.056	−1.047
3	0.2/0.02	−0.95	−1.080	−1.014	−1.030	−1.090
4	0.1/0.01	−1.25	−1.046	−1.037	−1.012	−1.266
5	0.05/0.005	−1.56	−1.036	−1.003	−1.000	−0.990
6	0.02/0.002	−1.95	−0.996	−0.988	−1.243	−0.976
7	0.01/0.001	−2.25	−1.090	−1.006	−0.992	−0.797

where as the receding contact angle (θ_r) determines the hydrophilic character of the surface, were performed at both left and right sides of each drop. In order to obtain reproducible results, no vibration and distortion of the drop was allowed during volume changes. Five readings were performed for each sample; the average value and standard deviation were calculated and reported in this study.

As the surface energy cannot be measured directly, different indirect methods have been proposed in the literature [13–15]. In this study, the harmonic-mean [13] and the geometric-mean [14,15] approximations

Table 13. Values of $\log (C_1+C_2)/2$ and permselectivity for $AlCl_3$, $FeCl_3$ electrolytes across molecularly imprinted (Isoproturon 2,4-D composite membrane) polymer membranes

			The values of permselectivity			
			$AlCl_3$		$FeCl_3$	
Sl. No.	Molar Conc.	$\log (C_1+C_2)/2$	Isoproturon	2,4-D	Isoproturon	2,4-D
1	1/0.1	−0.25	−0.994	−0.980	−0.957	−0.818
2	0.5/0.05	−0.56	−1.000	−1.000	−0.978	−0.982
3	0.2/0.02	−0.95	−1.001	−1.020	−0.981	−1.049
4	0.1/0.01	−1.25	−1.100	−1.028	−1.158	−1.230
5	0.05/0.005	−1.56	−1.107	−1.050	−1.012	−1.136
6	0.02/0.002	−1.95	−1.266	−1.082	−1.030	−1.146
7	0.01/0.001	−2.25	−1.107	−1.069	−1.010	−1.131

Table 14. The values of fixed charged density of LiCl, NaCl, KCl, $MgCl_2$, $CaCl_2$, $AlCl_3$ and $FeCl_3$ across molecularly imprinted (isoproturon membrane) polymer membranes

Sl. No.	Molar conc.	LiCl	NaCl	KCl	$MgCl_2$	$CaCl_2$	$AlCl_3$	$FeCl_3$
1	1/0.1	−1.220	−1.230	−1.237	−2.730	−3.030	−7.700	−6.90
2	0.5/0.05	−0.590	−0.614	−0.628	−1.420	−1.760	−0.550	−2.17
3	0.2/0.02	−0.255	−0.250	−0.254	−0.594	−0.921	−0.220	−1.05
4	0.1/0.01	−0.134	−0.132	−0.144	−0.383	−0.732	−0.264	−0.21
5	0.05/0.005	−0.680	−0.720	−0.680	−2.100	−0.028	−0.091	−0.31
6	0.02/0.002	−0.277	−0.029	−0.032	−0.200	−0.307	−0.053	−0.09
7	0.01/0.001	−0.013	−0.013	−0.014	−0.024	−0.210	−0.220	−0.72

were employed to get the dispersive and the non-dispersive contributions to the total surface energy.

Measurements of contact angles revealed that advancing and receding contact angles were greater at the MIP membrane. Table 1 shows the values of the surface energies and the degree of surface polarity calculated as the ratio of the non-dispersive surface energy to the total surface energy (γ_s^{nd}/γ_s). Generally, the variation of γ_s^{nd} values calculated using the geometric-mean equation agrees to those obtained from the harmonic-mean equation, but there are important quantitative differences. The values of γ_s^{d} calculated with the geometric-mean equation are higher compared to the harmonic-mean approximation while the γ_s^{nd} values obtained from the geometric-mean approximation are lower. The degree of surface polarity obtained is very small when the geometric-mean method is employed. The unimprinted (UM1,2) membranes had a relatively high (about 15%) non-dispersive, γ_s^{nd} component in comparison with MIP membranes, while the dispersive component, γ_s^{d}, for both the UM and MIP membranes were almost equal. This was shown by the geometric-mean and the harmonic-mean approximations.

From our results we can conclude that the MIP membrane surface is more hydrophobic due to the presence of imprinted binding sites. Moreover, an increased receding contact angle indicates that hydrophobic locks remain at the membrane surface when the surrounding medium changes between air and liquid.

3.4. Ion transport study

It is seen from Tables 2–4 which include measurements of membrane potentials of isoproturon and 2,4-D MIP membrane that as the concentration of the electrolytic solutions increase the membrane potential $\Delta\Phi$ goes through a maximum value and levels off, giving a negative slope. The results are in agreement within reasonable ranges either experimentally or theoretically with those in the literature [16–18]. It is obvious that the different parabolic curves are due to the Donnan potential effect [19]. In other words, co-ions are efficiently excluded from the membrane. Thus, counterions permeate membranes.

The result of study of transport ions with molecularly imprinted isoproturon and 2,4-D polymer membrane which are shown in Tables 5–7 give the values

Table 15. The values of fixed charged density of LiCl, NaCl, KCl, $MgCl_2$, $CaCl_2$, $AlCl_3$ and $FeCl_3$ across molecularly imprinted (2,4-D) polymer membrane

Sl. No.	Molar conc.	LiCl	NaCl	KCl	$MgCl_2$	$CaCl_2$	$AlCl_3$	$FeCl_3$
1	1/0.1	−1.222	−1.224	−1.381	−3.130	−3.390	−0.720	−1.500
2	0.5/0.05	−0.670	−0.633	−0.710	−1.660	−1.857	−0.550	−2.700
3	0.2/0.02	−0.244	−0.251	−0.299	−1.394	−0.553	−1.450	−0.696
4	0.1/0.01	−0.134	−0.139	−0.168	−0.410	−0.179	−0.474	−0.188
5	0.05/0.005	−0.072	−0.077	−0.093	−0.673	−0.380	−0.180	−0.10
6	0.02/0.002	−0.276	−0.031	−0.034	−0.330	−0.080	−0.576	−0.039
7	0.01/0.001	−0.013	−0.014	−0.017	−0.090	−0.030	−0.027	−0.021

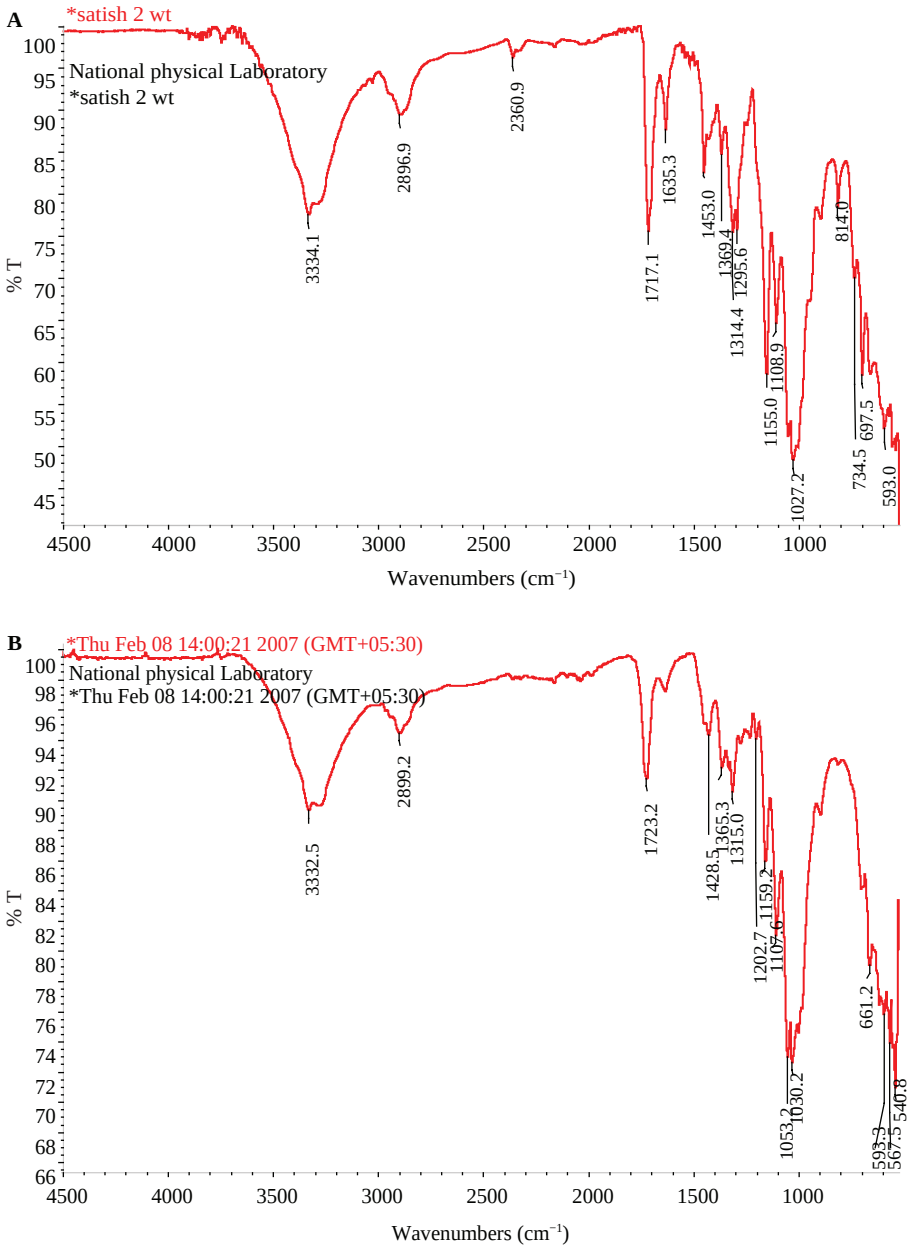

Fig. 2(a). FTIR spectra of polymer composite membrane with isoproturon template. (b). FTIR spectra of the isoproturon imprinted MIP membrane.

of transport number for LiCl, NaCl, KCl, $CaCl_2$, $MgCl_2$ $AlCl_3$ and $FeCl_3$ obtained by employing Eq. (4)–(6) using membrane potential data. It is evident from these tables that there is an initial increase in the transport number of co-ions as the concentrations of electrolytes is increased and then the values of transport number are variable.

The various values of permselectivity (Ps) and fixed charge density (Φx) calculated for LiCl, NaCl, KCl, $MgCl_2$, $CaCl_2$, $FeCl_3$ and $AlCl_3$ by substituting the value of α, ξ and t_+ in Eq. (9) given by Kobatake et al. [18]

$$\frac{1}{(4\xi^2+1)^{1/2}} = \frac{[1-t_+-\alpha]}{[\alpha-(2\alpha-1)(1-t_+)]} = \text{Ps}. \quad (9)$$

The various values of permselectivity (Ps) and fixed charge density (Φx) for LiCl, NaCl, KCl, $MgCl_2$, $CaCl_2$, $FeCl_3$ and $AlCl_3$ are summarized in Tables 11–13. The

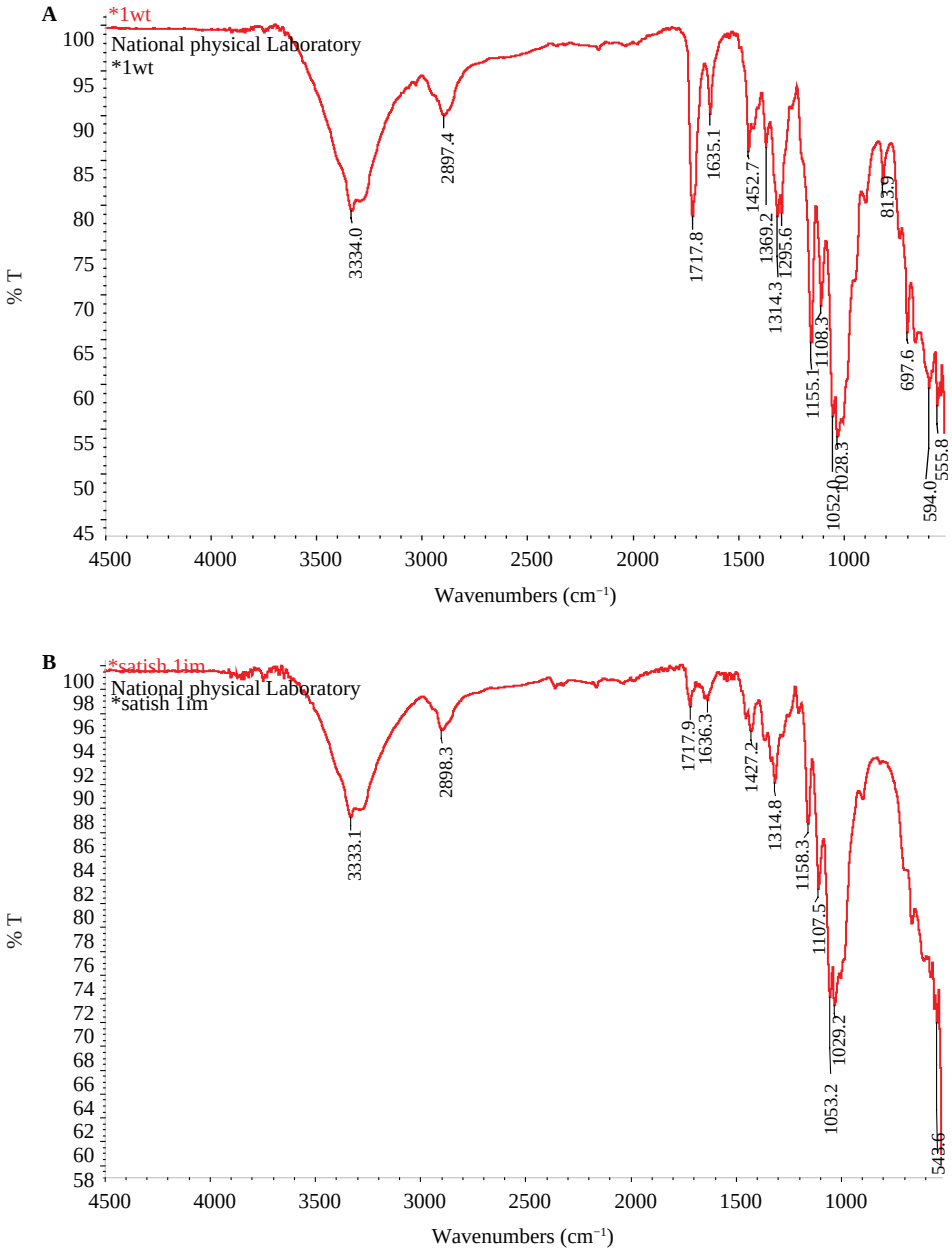

Fig. 3a. FTIR spectra of polymer composite membrane with 2,4-D template. (b). FTIR spectra of the 2,4-D Imprinted MIP membrane.

value of fixed charge density is shown in Tables 14 and 15.

The different values of α for LiCl, NaCl, KCl, $MgCl_2$ $CaCl_2$, $FeCl_3$ and $AlCl_3$ for each set of concentration can be calculated plotting the graphs between $1/t_+$ and $1/C_2$. The values of $1/t_+$ and $1/C_2$ are given in Tables 8–10 and these values are used for plotting the graph between $1/t_+$ and $1/C_2$. The intercept of the graph for all the electrolytes were put equal to $1/(1-\alpha)$ and using the different values of slope for the plots of LiCl, NaCl, KCl, $MgCl_2$, $CaCl_2$, $FeCl_3$ and $AlCl_3$ the values of permselectivity were calculated for the electrolytic concentrations using Eq. (9).

4. Discussion

The contact angles measurement reveals that both advancing and receding contact angles increased with the molecular imprinting (template removal of both isoproturon and 2,4-D imprinted membranes). Therefore, the MIP membrane surfaces were more hydrophobic. This result was attributed to the

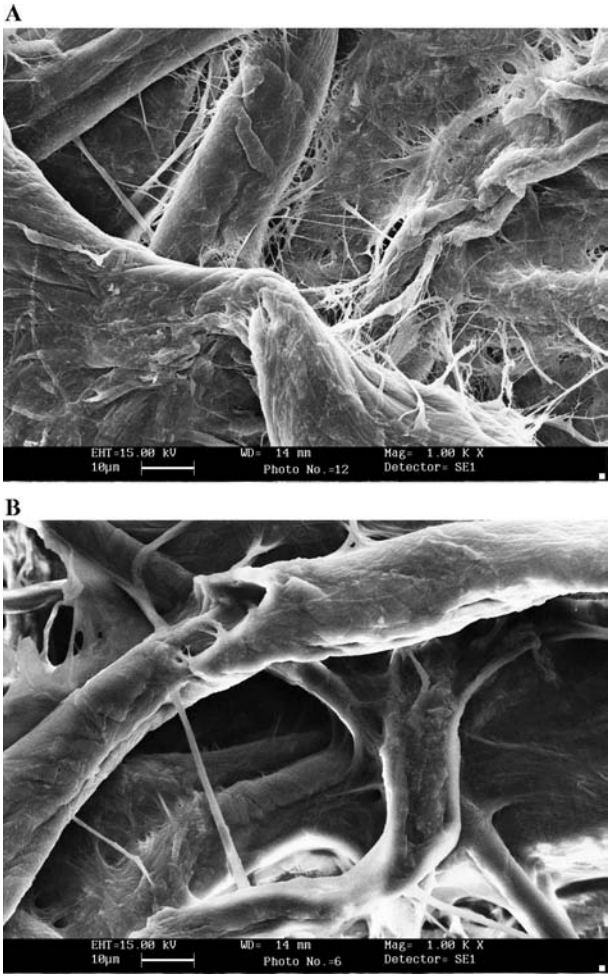

Fig. 4(a). SEM of isoproturon imprinted membrane. Micrograph is taken at magnification 1.00KX and resolution 10 μm at SEI detector. (b). SEM of 2,4-D imprinted membrane. Micrograph is taken at magnification 1.00KX and resolution 10 μm at SEI detector.

presence of imprinted binding sites of the membranes, and more directly to the hydrophobic nature of the MIP membrane surface. Furthermore, increase in the receding contact angle by the template removal from the surface of membranes indicates that hydrophobic locks remain at the membrane surface even after the surrounding of the surface changes from air to liquid.

Moreover, it was observed that the stability of the hydrophobic character was enhanced by increasing the amount of isoproturon and 2, 4-D templates. In order to evaluate the component surface energy of the unimprinted (with templates) and imprinted (after removal of templates) membranes, the harmonic-mean and geometric-mean approximations were used. Table 1 shows the values of the surface energies calculated using Eqs. (1)–(3) and the degree of surface polarity calculated as the ratio of the non-dispersive surface energy to the total surface energy (γ_s^{nd}/γ_s).

In general, the variation of γ_s^{nd} values calculated using the geometric-mean equation is the same as that obtained with the harmonic-mean equation, but there are important quantitative differences. These values are larger, 4–15%, when calculated with the geometric-mean equation compared with the harmonic-mean approximation, and the γ_s^{nd} values obtained from the geometric-mean approximation are smaller, 55–85%. Moreover, the degree of surface polarity obtained is very small when the geometric-mean method is used. The unimprinted UM_1 and UM_2 membranes had a relatively high non-dispersive, γ_s^{nd} component in comparison with MIP membranes (MIP_1 and MIP_2), while the dispersive component, γ_s^{d}, for both the UM and MIP membranes were almost equal. Both the geometric-mean and the harmonic-mean approximations reached the above conclusion.

4.1 Measurements of membrane potentials of isoproturon and 2,4-D MIP membrane

When the electrolyte concentration is increased, the Donnan exclusion has less effect, and thus co-ion uptake influence prevails. In the higher concentrations range of electrolytic solutions, the variations of diffusion membrane potential deviated from linearity. This discrepancy can be explained by consideration of classical theories developed by TMS [20–24] in order to account for the potentiostatic response of MIP membranes. The deviations from Nerstian responses are due to the penetration of co-ions into the membrane by osmotic effects and to diffusion of the electrolyte inside the membrane. The critical analysis of the data of these tables reveals that the values of membrane potential are increasing with decrease in concentration of LiCl, NaCl, KCl, $MgCl_2$, $CaCl_2$, $AlCl_3$ and $FeCl_3$ and then reaching to maximum value followed by a decrease of membrane potential values. The membrane potential developed seems to be in good resemblance with the ionic size and ionization energy of the ions i.e. $Li^+ < Na^+ < K^+$. Thus, Li^+ and Na^+ ions are more hydrated and move slower in transmembrane region exhibiting more membrane potential in comparison of K^+. Here the hydrated effect overcomes the size of ion. The membrane potential increases for LiCl, NaCl, KCl, $MgCl_2$, $CaCl_2$, $AlCl_3$ and $FeCl_3$ initially and then starts decreasing reaching to almost constant values. This phenomenon shows that MIP initially accumulates ions rapidly within transmembrane region due to which membrane potential increases after saturation within transmembrane it attains a steady state.

As far as transport number studies are concerned with different electrolytes, it is evident from Tables

5–7 that there is an initial increase in the transport number of co-ions as the concentrations of electrolytes is increased and then the values of transport number are variable. These results are in good resemblance of the observations made by Benevento [25] on membranes and clearly show that there is initial gathering of ions near the surface of MIP membrane and then quick leakage starts in the form of ions transport along with accumulation of ions within transmembrane region. This gathering and accumulation of ions (Li^+, Na^+, K^+, Ca^{++}, Mg^{++}, Al^{+++} and Fe^{+++}) is admissible.

Soon acquires the steady state and hence the almost constant values of transport is obtained the trend of initial decrease in transport number is more visible for lower electrolytic concentration than at higher concentration which also confirms the gathering and accumulation of ions near and across the MIP membrane, respectively.

The permselectivity (Ps) is a measure of selectivity of membrane electrolyte system and can be calculated from membrane potential data. The study of permselectivity and fixed charge density with molecularly imprinted isoproturon and 2,4-D polymer membrane indicated that when the average concentration $(C_1+C_2)/2$, becomes equal to effective fixed charge density, i.e. $C/\Phi_x = 1$, substituting the value of $\varepsilon = 1$ in $Ps = (1+4\varepsilon^2)^{-1/2}$ the Ps becomes equal to 0.448, the corresponding concentration were obtained from the Ps vs log $(C_1+C_2)/2$ plots. The concentration should be equal to the fixed charged density for various electrolytes. Since the values of Ps should be 0.448 but it is apparent from all of these figures that this magic value is rare in almost all of the plots. Thus this may be possible denial of the applicability of this method with MIP membrane because after the removal of isoproturon template this magic value may have changed and therefore this method does not holds good for these MIP membranes which may be fruitful for the computational characterization of MIPs [26]. One of the possible reasons of this denial of this applicability may be that porosity of membrane is generally generated with the formation of membrane matrix while in this case the removal of template causes some sort of extra porosity after formation of membrane which is not uniform on the both surfaces of membrane and in membrane matrix as well. Further molecularly imprinted polymer (MIPs) are becoming the wide range of artificial recognition sites in sensors and separation technology [27–29], hence their ion transport study could be one of the tools for their proper characterization.

5. Conclusion.

The robustness and specificity of the MIPs membranes are the basis of their wide applicability in various fields. These membranes are widely used in separation and sensing technologies. MIP membranes have additional porosity and surface diversity in comparison of other membranes due to later removal of templates. Only a little is known about their transport study. Thus present piece of work defines their characterization through ion transport study by calculating membrane potential, transport number, permselectivity and fixed charge density along with contact angle measurement. The 2,4-D and isoproturon imprinted membranes were prepared and characterized using the principle of irreversible thermodynamics and various theories were tested with these membranes. The ion transport number, perm selectivity and fixed charge density were calculated for LiCl, NaCl, KCl, $MgCl_2$, $CaCl_2$, $AlCl_3$ and $FeCl_3$ by substituting the values of membrane potential in their respective equations from membrane potential data. These membranes show the applicability of irreversible thermodynamical theories of ion transport with some exceptional denial.

Reference

[1] G. Wulff, Angew. Chem., Int. Ed. Engl., 34 (1995) 1812–1832.
[2] K. Haupt, K. Mosbach, Biochem. Soc. Trans., 27 (2) (1999) 344–350.
[3] B. Sellergren, Trends Anal. Chem., 16(6) (1997) 310–320.
[4] K. Hosoya and N. Tanaka, ACS Symp. Ser., 703 (1998) 143–158.
[5] T. Takeuchi and J. Haginaka, J. Chromatogr. B, 728(1) (1999) 1–20.
[6] Q. Liu, Y.X. Zhou and Y.T. Liu, Chin. J. Anal. Chem., 27(11) (1999) 1341–1347.
[7] F.L. Dickert, P. Lieberzeit, and M. Tortschanoff, Sens. Actuat. B: Chem. 65(1–3) (2000) 186–189.
[8] T.A. Sergeyeva, S.A. Piletsky, A.A.; Slinchenko, L.A.; Sergeeva and L.M. El'skaya, Anal. Chim. Acta, 392 (1990) 105.
[9] T.A. Sergeyeva, H. Matuschewski, S.A. Piletsky, J. Bending and U. Schedler, M.J. Ulbricht, Chromatography A, 89 (2001) 907.
[10] M. Yoshikawa, J. Izumi, T. Kitao,; S. Koya and S. Sakamato, J. Membr. Sci., 108 (1995) 171.
[11] M. Stahl, M.O.;Manson and K. Mosbach, Biotechnol. Lett., 12 (1990) 161.
[12] K.P. Singh, S. Ahalawat, R.K. Prajapati, S. Kumar, P. Singh and S.K. Dhawan, Ionics (2010) DOI 10.1007/s11581-010-0419-0.
[13] S. Wu, Polymer Interface and Adhesion, Marcel Dekker, New York, 1982.
[14] D.K. Owens and R.C. Wendt, J. Appl. Polym. Sci., 13 (1969) 1741–1747.
[15] K.L. Mittal, Contact Angle, Wettability and Adhesion, VSP,Utrecht, The Netherlands, 1993.
[16] V. Compan, T.S. Sorensen and S.R. Rivera, J. Phys. Chem., 99 (1995) 12553–12558.
[17] T.S. Sorensen and V. Compan, J. Phys. Chem., 100 (1996) 7623–7631.
[18] K. Singh and V.K. Shani, Indian J. Chem., 28A (1989) 1084.
[19] Y. Kobatake and N. Kamo, Prog. Polym. Sci. Jpn,, 5 (1972) 257.
[20] T. Teorell, Proc. Natl. Acad. Sci, U.S.A., (1935) 21152.
[21] K.H. Meyer and J.F. Siever, Hel. Chem. Acta., 19 (1936) 987.
[22] T. Teorell, in Progress of Biophysics, Butler and Randoll (Eds.), Academic Press. New York, Vol. 3, 1953, p. 305.
[23] R. Schlogl, Z. Electrochem., 57 (1953) 195.
[24] R. Schlogl, Z. Physik. Chem., (Frankfurt) (1954) 1305.
[25] J. Benavente, J. Non-Equlib. Thermodyn., 9 (1984) 217.

[26] Y. Liu, F. Wang, T. Tan and M. Lei, Anal. Chim. Acta., 581 (2007) 137–146.
[27] T. Alizadeh, M. Zare, M.R. Ganjali, P. Norouzi, and B. Tavana, Biosens. Bioelectron., 25(5) (2009) 1166–1172.
[28] T. Alizadeh and M. Akhoundian, Electrochimica Acta, 55 (10) (2010) 3477–3485.
[29] S.J. Ahmadi, O. Noori-Kalkhoran and S. Shirvani-Arani, J. Hazard. Mater., 175 (1–3) (2009) 193–197.